Time-dependent Nonlinear Optical Properties of Pyroelectric Liquid Crystalline Polymers

Jonas Örtegren[1], Philippe Busson[1], Ulf W. Gedde[1]*, Anders Hult[1], Anders Eriksson[2], Mikael Lindgren[2,3], Per-Otto Arntzén[3], David S. Hermann[4], Per Rudquist[4], Sven T. Lagerwall[4]

1. Department of Polymer Technology, Royal Institute of Technology, SE-100 44 Stockholm, Sweden
2. Department of Physics, Linköping University, SE-581 83 Linköping, Sweden
3. National Defence Research Establishment, P.O. Box 1165, SE-581 11 Linköping, Sweden
4. Physics Department, Chalmers University of Technology, SE-412 96 Göteborg, Sweden

SUMMARY: Highly oriented pyroelectric liquid-crystalline polymers were prepared by photopolymerization under the influence of a static electric field from binary mixtures of two acrylate monomers exhibiting chiral smectic C mesomorphism. Both monomers contained nitro groups to yield second order nonlinear optical properties (second harmonic generation) and one of the monomers had two functional groups to yield a crosslinked polymer. The room temperature second order nonlinear susceptibility of the polymers showed during the first two hours a 10 % decrease after which it remained constant during the next 48 days. At elevated temperatures there was a significant difference in the nonlinear optical properties over time between crosslinked and uncrosslinked polymers. The uncrosslinked polymer showed a pronounced loss of second order nonlinear optical activity with time at ≥38°C. The crosslinked polymer showed a much smaller and basically a temperature independent decrease rate in the second order nonlinear optical properties at all the ageing temperatures (23-130°C). Both the loss in mesogen order parameter, very evident for the uncrosslinked polymer, and conformational changes occurring within the mesogens (β mechanism), may account for the observations made.

(Keywords: pyroelectric liquid crystalline polymers, second harmonic generation, long-term properties)

* To whom correspondence should be addressed

© WILEY-VCH Verlag GmbH, D-69469 Weinheim, 1999 CCC 1022-1360/99/$ 17.50+.50/0

Introduction

New materials for integrated optics, particularly polymeric materials for active waveguides, have received considerable attention in recent years. The main advantages of using polymers in active waveguides are their good processability, possibility for integration with passive polymeric waveguides, and their potentially high nonlinear optical (NLO) susceptibility. Important fields of application are frequency-conversion devices and electro-optic modulators[1]. The commercial acceptance of these materials will, among other factors, be determined by their long-term operational stability[2]. One approach of making organic materials with satisfactory NLO susceptibility is to electrically pole amorphous polymers in a state where the nonlinear optical moieties, which are incorporated (blended or chemically bonded) into the polymer, rotate through the coupling of the dipole to an applied electric field. After the alignment of the dipoles, the polymer is cooled into its glassy state, where the dipole rotation is greatly retarded. The long-term properties of such materials have been studied, and one of the factors that improve the long-term stability is crosslinking[3-5]. We have used a different approach to make materials with non-linear optical properties. Ferroelectric liquid crystals have been aligned and photopolymerized in a static electric field. These polymers are denoted "pyroelectric" because the dipoles show no apparent reorientation on a polarity switch of the external electric field[6].

This paper reports data on the time evolution during 50 days of the second-order NLO susceptibility of poled, uncrosslinked and crosslinked pyroelectric liquid-crystalline polymers. The second order NLO susceptibility was obtained by measurement of the second harmonic generation (SHG). The polymers showed only a moderate decrease in the NLO properties with time at room temperature. At elevated temperatures, however, the uncrosslinked polymer showed a considerable stronger and faster deterioration of the NLO properties than the crosslinked polymer.

Experimental

The two chiral monomers **A1b** and **A2c** (Figure 1), exhibiting chiral smectic C (s_C^*) - mesomorphism, were synthesized according to methods reported elsewhere[7,8]. High-pressure liquid chromatography showed that the purity of the monomers was 97% (**A1b**) and 96% (**A2c**). Monomer **A1b** and a mixture of 80% **A1b** and 20% **A2c** (molar ratio) were blended with 2 weight-% of the photoinitiator TPO lucirin (Figure 2). The polymers synthesized are hereafter referred to as poly(**A1b**) and poly(**A1b**/**A2c**). Methylene chloride was used as solvent during the mixing of the constituents, and the preparations were conducted under yellow light in order to prevent early polymerization of the monomers. Differential scanning calorimetry (Mettler-Toledo DSC 820) and polarized light microscopy (Leitz Ortholux POL BK II) were used to determine the phase transitions in the monomer mixtures.

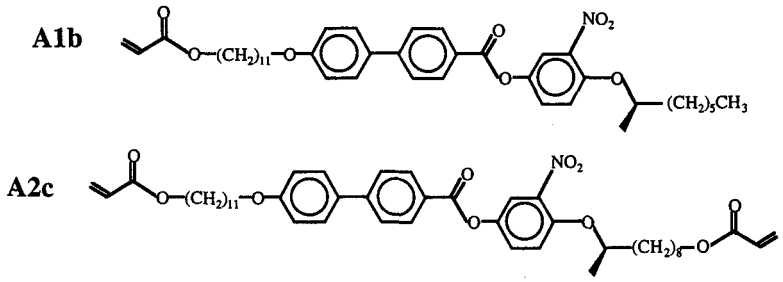

Figure 1. Structure of monomers used.

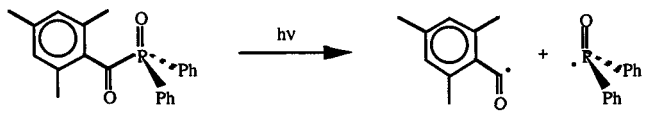

Figure 2. UV-induced decomposition of the photoinitiator TPO.

Commercial 4 μm glass cells (EHC, Japan) with both sides pretreated with indium tin oxide (ITO) and rubbed polyimide, where the polyimide enhanced planar alignment of the molecules, were used for the film preparation. The blends were heated to 70-80°C, which is above the isotropization temperature, and at this temperature the monomer liquids were soaked into the glass cell by capillary forces. The samples were cooled from the isotropic phase down to the s_C^*-phase while being exposed to a 20 V/μm electric field along the

normal to the film. The photopolymerizations were carried out at 33 to 35°C for 20 min using a Luxor UV-polymerization unit. Infrared spectroscopy (Spectrum 2000, Perkin-Elmer) showed that these conditions enabled complete polymerization. No traces of unreacted acrylate groups (absorption bands: 1408 cm^{-1} and 1638 cm^{-1}) were detected.

The "short-term" NLO properties (1-2 h) were obtained by continuous measurements of the SHG light power at a fixed combination of incidence and azimuthal angles directly after polymerization and release of the electrical field. The temperature was controlled within ±1°C by tuning a heat pistol in front of the samples.

On measuring the "middle-term" properties (<10 h) some of the samples from the short-term measurements were used, and some new samples were made. The "middle-term" SHG light power measurements were carried at room temperature on samples aged at different temperatures in a Mettler Hot Stage FP 82. The measurements were carried out after different ageing times over a wide range of incidence and azimuthal angles.

The "long-term" data (≤50 days) were obtained by measurements of the SHG light power at room temperature on samples aged at room temperature. The measurements were carried out over a wide range of incidence and azimuthal angles.

The set-up used for the measurements of the SHG light power are schematically shown in Figure 3. A pulsed Nd:YAG laser with a wavelength of 1064 nm at a pulse repetition frequency of 10 Hz with a pulse width of approximately 4 ns was used as the light source (pump beam). Appropriate intensity (~46-48 μJ/pulse) and frequency was obtained by adjusting optical density filters, a cold mirror and a polarizer. Part of the intensity was extracted by a beam splitter and detected with an InGaAs-pin diode as a reference. A 400 mm lens focused the pump beam onto the sample. The sample was possible to rotate about two axes using two rotation stages controlled by a Newport MM 2000 unit. The power of the SHG light was, after first passing a 45° hot mirror and a narrow-band-width-interference filter, recorded by a photomultiplier tube (Hamatsu 5783-01). The recorded power was obtained as the average of four or sixteen pulses. The signals of the reference detector and the photomultiplier tube were collected using a Lecroy 9360 oscilloscope and transferred to a pc.

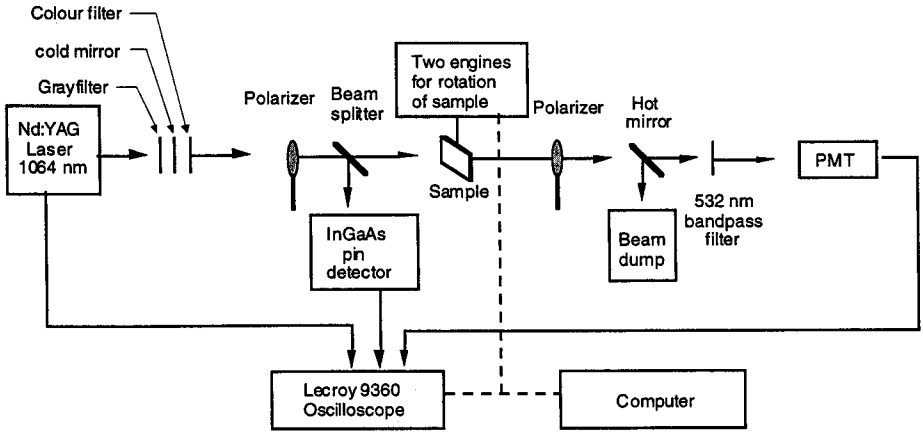

Figure 3. The experimental setup for the second harmonic generation measurements.

The C_2-point group symmetry (Schoenflies notation) of the NLO polymers was identified by measuring the SHG power as a function of the azimuthal angle for a fixed angle of incidence. The d-coefficients of the second order non-linear susceptibility of the samples were determined by proper choice of azimuthal angle and secondly by making SHG light power measurements over a range (-30° to +30°) of angle of incidence. The short-term NLO behaviour was recorded by measuring the SHG light power at a fixed combination of incidence and azimuthal angles, at which the d_{23}-coefficient gave a large contribution to the SHG power. The laser light was continuously pumped onto the sample and the SHG light power was measured continuously. Calculations of the d-coefficients were made using a Matlab least-squares-fit program for a chosen azimuthal angle. Z-cut 530 nm lithiumniobate (point group C_{3v}) was used as a reference. The refractive index was determined at 632.8 nm by m-line spectroscopy and the birefringence was measured using a Leitz Ortholux POL BK II microscope equipped with crossed polarizers and a Leitz tilting compensator B[9].

Calculations

The transmitted second harmonic power of light $P_{2\omega}$ for a fixed azimuthal angle is given by[1]:

$$P_{2\omega} = \frac{m}{n(\theta)_{2\omega} n(\theta)_{\omega}^2} \left[\frac{d(\theta) P_{\omega}}{\lambda_0} \frac{l_0}{\cos\theta} \right]^2 \frac{\sin^2 \left[\frac{2\pi}{\lambda_0} \frac{l_0}{\cos\theta} (n(\theta)_{\omega} - n(\theta)_{2\omega}) \right]}{\left[\frac{2\pi}{\lambda_0} \frac{l_0}{\cos\theta} (n(\theta)_{\omega} - n(\theta)_{2\omega}) \right]^2} \quad \ldots(1)$$

where P_{ω} is the incoming power of light, $n(\theta)_{\omega,2\omega}$ is the refractive index at the specific frequency, l_0 is the sample thickness and $l_0/\cos\theta$ the length of interaction, λ_0 is the wavelength of the incoming light, and m is a constant relating to the experimental set-up. θ is related to the angle of incidence θ_{in} as described below. The constant m was obtained by measuring the second harmonic power of 530 μm z-cut lithiumniobate ($LiNbO_3$) whose effective d-coefficient d_{eff} for ps-polarization (i.e. the plane-polarized incoming wave was parallel to the plane of incidence, and the plane-polarized outgoing wave was perpendicular ('senkrecht') to the plane of incidence) is given by:

$$d_{eff} = d_{22} \cos^2\theta \cos\phi (3\sin^2\phi - \cos^2\phi) \quad \ldots(2)$$

where ϕ is the azimuthal angle. The following values were used for the calculations[10]: $d_{22} = 2.76$ pm/V, $n_{\omega,o} = 2.234$ $n_{\omega,e} = 2.1554$ $n_{2\omega,o} = 2.3251$ and $n_{2\omega,e} = 2.233$. The C_{3v} point group symmetry was identified experimentally, and the SHG power was measured as a function of the angle of incidence at $\phi = 0°$.

The polymer samples were assumed to be uniaxial, an assumption confirmed by m-line spectroscopy measurements on the aged pyroelectric polymers[9]. The coordinate system denoted (**x**,**y**,**z**) (Figure 4) is a coordinate system oriented along the dielectric axis of the film. Axes **x** and **z** were assumed to lie in the plane of the film, **z** being the optical axis and **y** the polar axis, normal to the surface. The laboratory coordinate system is denoted (**X**,**Y**,**Z**), where **Y** and **Z** are the horizontal axes and **X** is the vertical axis. ϕ is the azimuthal angle, i.e. the angle between **z** and **Z** and θ_{in} is the angle of incidence for rotation around **Z**. The light propagated along **Y**. The calculation of the d_{23}-coefficient (p-p polarization; two

extraordinary pump waves form one second harmonic extraordinary wave) was performed in the following way. The effective d-value (d_{eff}) for a material showing C_2 symmetry with the polar axis along y and with the incident and azimuthal angles defined according to Figures 4 and 5 is given by[11-13]:

$$d_{eff} = \bar{p}_{2\omega,e} \circ \bar{\bar{d}} \otimes \bar{p}_{\omega,e} \bar{p}_{\omega,e} \qquad \ldots(3)$$

where $\bar{p}_{2\omega,\omega,e}$ is a unit vector given by equation (4).

$$\bar{p}_{2\omega,\omega,e} = \left[\cos\theta_{2\omega,\omega,o}\cos\phi \quad \sin\theta_{2\omega,\omega,o} \quad \cos\theta_{2\omega,\omega,e}\sin\phi\right] \qquad \ldots(4)$$

Equation (3) in contracted notation and under Kleinman symmetry conditions[14], is written in expanded form in the following way:

$$d_{eff} = \bar{p}_{2\omega,e}\begin{bmatrix} 0 & 0 & 0 & d_{14} & 0 & d_{16} \\ d_{16} & d_{22} & d_{23} & 0 & d_{14} & 0 \\ 0 & 0 & 0 & d_{23} & 0 & d_{14} \end{bmatrix}\begin{bmatrix} \bar{p}_{\omega,e}(1,1)^2 \\ \bar{p}_{\omega,e}(1,2)^2 \\ \bar{p}_{\omega,e}(1,3)^2 \\ 2\bar{p}_{\omega,e}(1,2)\bar{p}_{\omega,e}(1,3) \\ 2\bar{p}_{\omega,e}(1,3)\bar{p}_{\omega,e}(1,1) \\ 2\bar{p}_{\omega,e}(1,1)\bar{p}_{\omega,e}(1,2) \end{bmatrix} \qquad \ldots(5)$$

where $\phi = 90°$, $\theta_{o,\omega}$ and $\theta_{e,\omega}$ are the angles between the surface-normal of the film and the **k**-vector of the fundamental ordinary and the extraordinary wave, respectively, and $\theta_{o,2\omega}$ and $\theta_{e,2\omega}$ are the angles between the surface-normal and the **k**-vector of the second harmonic ordinary and the extraordinary wave, respectively. These angles differ from θ_{in} and were obtained using Snell's law:

$$\sin(\theta_{in}) = n_{2\omega,\omega,e}(\theta_{2\omega,\omega,e})\sin(\theta_{2\omega,\omega,e}) \qquad \ldots(6)$$

and the ellipsoidal refractive index equation of a uniaxial material (Figure 5):

$$\frac{x^2}{n_{2\omega,\omega,o}^2} + \frac{y^2}{n_{2\omega,\omega,o}^2} + \frac{z^2}{n_{2\omega,\omega,e}^2} = 1 \qquad \ldots(7)$$

where $(x,y,z) = n(\theta_{2\omega,\omega,e})(0,\sin(\theta_{2\omega,\omega,e}),\cos(\theta_{2\omega,\omega,e}))$

Insertion of equation (7) in equation (6) yields:

$$\theta_{2\omega,\omega,e} = \arctan\left(\frac{n_o \sin\theta_{in}}{\sqrt{n^2_{2\omega,\omega,e} n^2_{2\omega,\omega,o} - n^2_{2\omega,\omega,e}\sin^2\theta_{in}}}\right) \quad \ldots(8)$$

By combining equations (4) and (5), the following expression is obtained:

$$d_{eff} = d_{22}\sin^2\theta_{\omega,o}\sin\theta_{2\omega,o} + d_{23}(\cos^2\theta_{\omega,e}\sin\theta_{2\omega,o} + 2\sin\theta_{\omega,o}\cos\theta_{\omega,e}\cos\theta_{2\omega,e}) \quad \ldots(9)$$

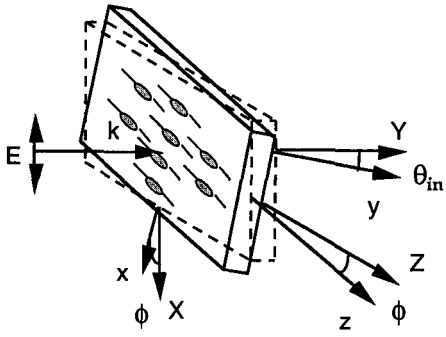

Figure 4. The definition of the coordinate system for the SHG measurements. z is parallel to the mesogens.

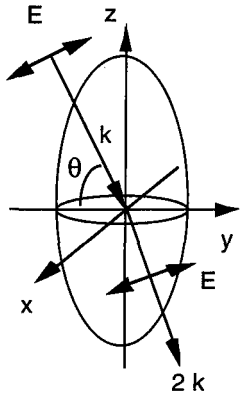

Figure 5. The geometry of the refractive index ellipsoid and the definition of the coordinate system used in this context. $\phi = 90°$ gives ee-e waves as all three E-field vectors are in the yz-plane (pp-polarization).

The refractive indices were obtained from data of Lindgren *et al.*[9]: $n_{\omega,e} = 1.63$; $n_{2\omega,e} = 1.64$; $n_{\omega,o} = 1.53$; $n_{\omega,e} = 1.54$. The refractive index of the glass was determined to $n_g = 1.5175$ by Abbe refractometry. For poled polymer films with axial symmetry (poling axis along z) there is a relation between two of the tensor components: $d_{33} = 3d_{13}$. In order to simplify the analysis the same relation was taken for the polar orientation in our polymer system (poling axis along y): $d_{22} = 3d_{23}$.

Results and Discussion

The data for the SHG light power as a function of the azimuthal angle ϕ were used to determine the principal axes of the nonlinear polarizability (Figure 6). In the plane of the glass cell, the principal axes were rotated between 15 to 30°, with respect to the rubbing direction of the polyimide alignment layer (Figure 6).

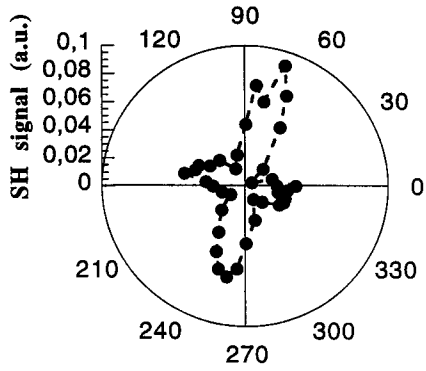

Figure 6. The C_2 point group of the NLO polymer, where the SHG light power was measured as a function of the azimuthal angle, ϕ, for an angle of incidence, θ_{in}, of 30° and pp-polarization.

The calculation of the *d*-coefficients of the second order nonlinear susceptibility matrix of the polymers was made by first taking the SHG light power data for the actual polymer (Figure 7). Then the SHG light power (as a function of angle of incidence) of $LiNbO_3$ with known *d*-coefficients was recorded (Figure 8). This procedure made it possible to convert the SHG light power data obtained for the polymer sample to *d*-coefficients. The coefficients d_{23} and d_{16} obtained for the NLO polymers were in the range 0.12-0.25 pm/V and 0.05-0.10 pm/V, respectively. Local variation in order parameter within specimens and between different specimens accounts for the scatter in the obtained *d*-values.

The SHG light power measurements were carried out first, before and after polymerization, with a 20 V/μm electric field acting on the sample. It turned out that SHG light power was slightly larger for the polymers than for monomer mixtures. The E-field was then switched off, which led to a pronounced decrease in the power of the SHG light. The decrease in the *d*-coefficients (proportional to the square root of the SHG light power) was approximately 50% at room temperature and even greater at higher temperatures (Figures 9-10). A substantial part of this loss was probably due to cancellation of the third-order optical nonlinearity

$\chi^{(3)}(-2\omega;\omega,\omega,0)$ originating from the static electric field. As the E-field was removed, the response was truly second order (i.e. $\chi^{(2)}(-2\omega;\omega,\omega)$). It is very possible that a part of the instantaneous loss accompanying the switch off of the E-field is due to a rapid decrease of the mesogen order parameter and reorientation of nitro-group dipoles. It is not possible, on the basis of the obtained data, to calculate the relative contribution from this process. The principal axes of the nonlinear susceptibility remained unchanged on polymerization and also on the removal of the E-field.

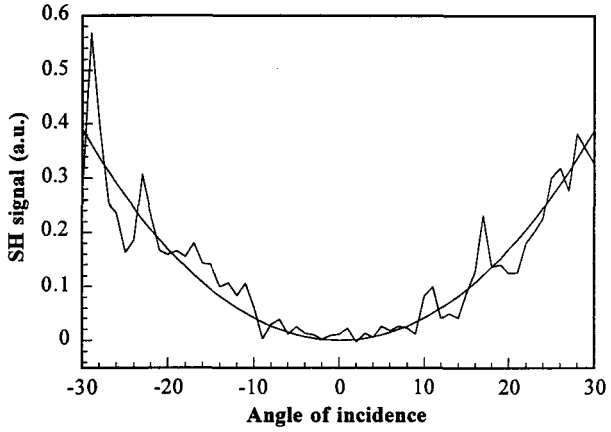

Figure 7. SHG light power versus angle of incidence for the 4 μm NLO polymer using pp-polarization and ee-e waves.

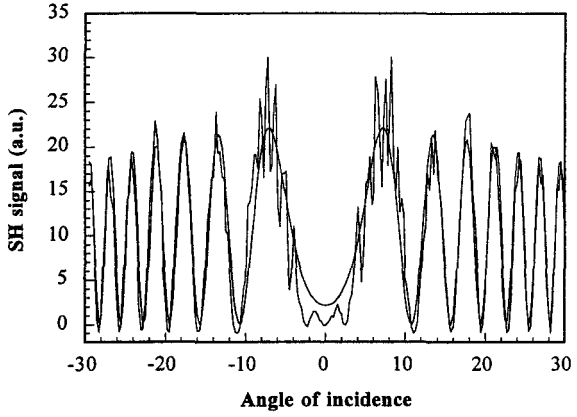

Figure 8. SHG light power versus angle of incidence for 531 μm $LiNbO_3$ using ps-polarization and ee-o waves.

The following equation was fitted to the time (t) dependence of the nonlinear susceptibility:

$$d = d_1 e^{-\frac{t}{\tau_1}} + d_2 \qquad \ldots(10)$$

where $\sum_{i=1}^{2} d_i = 1$. Note that the d-values given in equation (10) were normalized with respect to the initial d-value ($d(0)$= 1) attained precisely after the switch-off of the E-field. Differences in the starting d-value existing for the different samples had by this procedure no influence on the time evolution of data. The coefficient d_2 is the time-independent part of the nonlinear susceptibility. The relaxation times τ_1 were obtained by fitting of equation (10) to the short-term data of the susceptibility. The middle-term data were taken at room temperature after ageing at different temperatures. This made the mathematical treatment of these data less meaningful and for this reason the d_i values presented in Tables 1 and 2 were based only on the short-term susceptibility data.

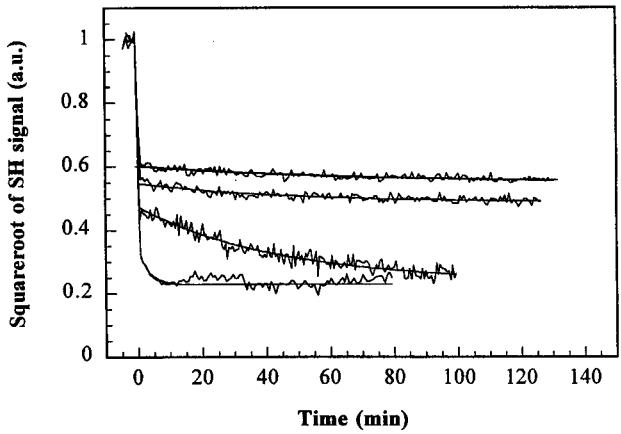

Figure 9. The time-dependence of the square root of the SHG power of poly(**A1b**) at 23, 31, 38 and 45°C (top-to-bottom). The electric field was removed at t=0. The continuous lines were obtained by fitting equation (10) to the experimental data.

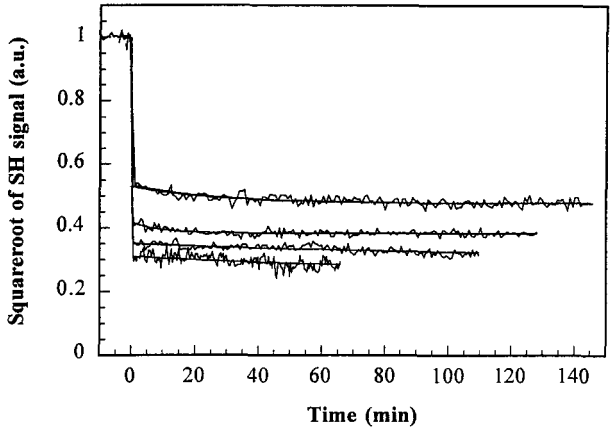

Figure 10. The time-dependence of the square root of the SHG power of poly(**A1b/A2c**) at 23, 68, 85 and 97°C (top-to-bottom). The electric field was removed at t=0. The continuous lines were obtained by fitting equation (10) to the experimental data.

Figures 9 and 10 show the short-term nonlinear optical susceptibility data. The uncrosslinked polymer displayed a very pronounced decrease in the SHG light intensity with time at temperatures ≥ 38°C (Figure 9). The crosslinked polymer showed only a small decrease in SHG light intensity with time during the first two hours (Figure 10). The temperature dependence (23-130°C) of the relaxation process was negligible for the crosslinked polymer (Figure 10). The relaxation process was adequately described by the single exponential expression (equation (10)). The optimum values for the adjustable parameters obtained by fitting equation (10) to the experimental short-term data are shown in Tables 1 and 2. The uncrosslinked polymer poly(**A1b**) showed a pronounced decrease in d_2 already at 38°C whereas d_2 remained practically constant and independent of temperature for the crosslinked polymer poly(**A1b/A2c**). The relaxation times obtained showed no real temperature trend for the crosslinked polymer whereas it decreased with increasing temperature for the uncrosslinked polymer.

Table 1. Fitted parameters (equation (10)) of poly(**A1b**)

Temperature (°C)	d_1	d_2	τ_1 (min)
23	0.09	0.91	70
31	0.11	0.89	45
38	0.50	0.50	43
45	0.33	0.67	3.2

Table 2. Fitted parameters (equation (10)) of poly(**A1b/A2c**)

Temperature (°C)	d_1	d_2	τ_1 (min)
23	0.10	0.90	25
68	0.08	0.92	10
85	0.10	0.90	85
97	0.11	0.89	45

The middle-term data shown in Figures 11 and 12 are basically in accordance with the short time data presented in Figures 9 and 10. The uncrosslinked polymer showed a pronounced loss in the second order non-linear optical susceptibility at ≥38°C whereas for the crosslinked polymer at all the ageing temperatures (23-130°C) it only showed a negligible (within 10%) decrease between 1 and 10 hours of ageing. The larger scatter in the middle-term data, in a comparison with the short-term data, was due to that each sample was repositioned in the optical set-up before each optical measurement. The middle-term relaxation data of poly(**A1b**) were different from those taken under in-situ conditions (short-term data); cf. Figures 9 and 11. It seems that the cooling of this polymer to room temperature caused changes in the morphology that had an impact on the NLO properties.

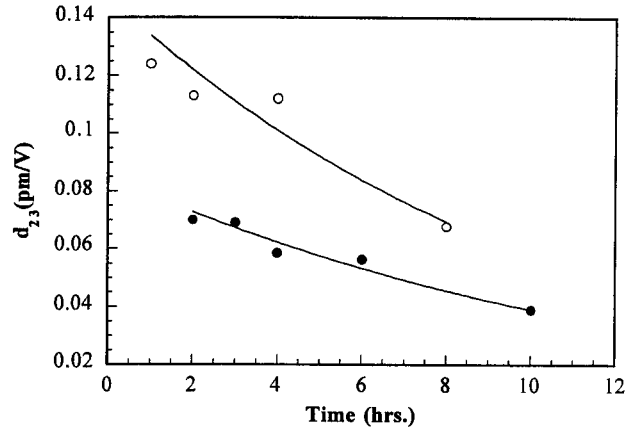

Figure 11. The nonlinear susceptibility (d_{23}) of poly(**A1b**) as function of ageing time at 38°C (upper) and 45°C (lower).

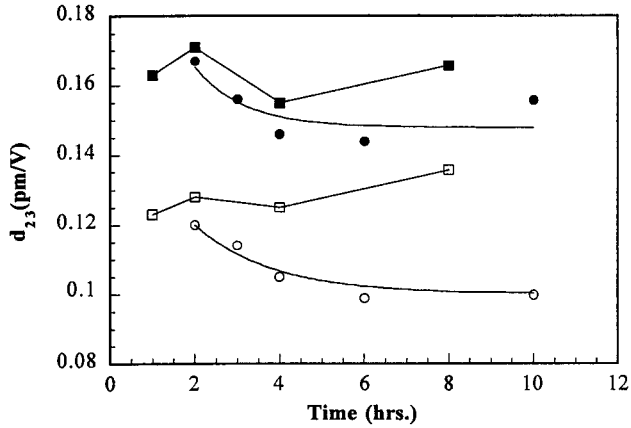

Figure 12. The nonlinear susceptibility (d_{23}) of poly(**A1b/A2c**) as function of ageing time. The ageing temperatures are from bottom to top: 68, 100, 85 and 130°C. The lines and curves are guides to the eye only.

At room temperature the d_{23}-value of the NLO susceptibility matrix of poly(**A1b**) was stable over 50 days (Figure 13). These data are thus in accordance with the short-term data shown in Figure 10. The crosslinked polymer (poly(**A1b/A2c**)) showed also a stable d_{23} over the 50 days.

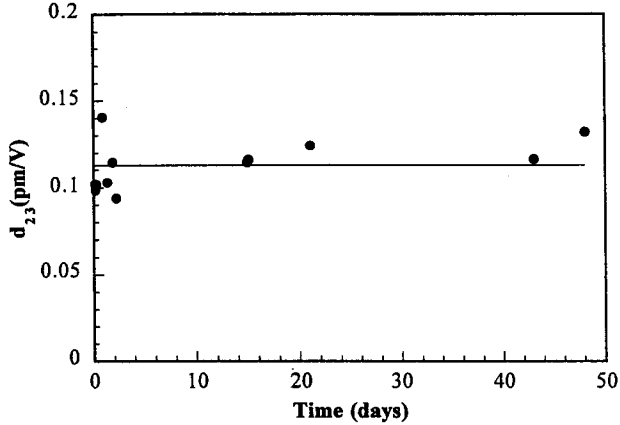

Figure 13. Non-linear optical susceptibility d_{23} of poly(**A1b**) as a function of ageing time at room temperature. The line is a guide to the eye only.

The birefringence colour of the uncrosslinked polymer (poly(**A1b**)), viewed in the polarized microscope, changed irreversibly from red to white as the temperature was raised above 45°C. This finding indicates an irreversible decrease in the order parameter at the higher temperatures which indeed is sufficient to explain the decrease in nonlinear susceptibility occurring at the higher temperatures. The crosslinked polymer (poly(**A1b/A2c**)) shifted reversibly from red to yellow between 70°C and 120°C and to white above 150°C. Even after having passed 200°C the crosslinked polymer retained its initial reddish colour at room temperature.

Except for chemical degradation[15,16], there are two processes that account for the loss in the NLO susceptibility on ageing: a decrease of the mesogen order parameter and a loss of polar order due to subglass-processes. The subglass process (β process) causes a 180° torsion of the phenyl group containing the nitro group without a change in the orientation of the mesogens[17,18]. However, dielectric data indicated that the relaxation strength of the β process in poly(**A1b**) and poly(**A1b/A2c**) is very small[17]. The loss in mesogen order parameter detected by polarized microscopy was more evident in poly(**A1b**) but also observed in poly(**A1b/A2c**) should be a prime factor explaining the loss in second order nonlinear optical susceptibility. Loss of susceptibility due to the β process can not be ruled out.

Conclusions

The time dependence of the second-order nonlinear optical (NLO) properties of uncrosslinked and crosslinked pyroelectric liquid crystalline polymers (PLCP) was studied. The room temperature second order nonlinear susceptibility of the polymers showed during the first two hours a 10 % decrease after which it remained constant during the next 48 days. At elevated temperatures there was a significant difference in the nonlinear optical properties over time between crosslinked and uncrosslinked polymers. The uncrosslinked polymer showed at ≥38°C a pronounced loss of second order nonlinear optical activity with time. The crosslinked polymer showed at all the ageing temperatures (23-130°C) a much smaller and basically a temperature independent decrease rate in the second order nonlinear optical properties. Both the loss in mesogen order parameter, very evident for the uncrosslinked polymer, and conformational changes occurring within the mesogens (β mechanism), may account for the observations made.

Acknowledgements

Financial support from the Swedish Research Council for Engineering Sciences (TFR), Defence Material Administration (FMV), Swedish Natural Science Research Council (NFR; grant K-AA/KK01910-311) and the Swedish National Foundation for Strategic Research is gratefully acknowledged. Drs. F. Sahlén and M. Trollsås, Department of Polymer Technology, Royal Institute of Technology, are thanked for the preparation of the monomers.

References

1. P.N. Prasad, D. J. Williams, *Introduction to Nonlinear Effects in Molecules and Polymers*, Wiley, New York 1991
2. D. R. Robello, C. S. Willand, M. Scozzafava, A. Ullman, D. J. Williams, in: *Materials for Nonlinear Optics - Chemical Perspectives, ACS Symposium Series 455*; S. R. Marder, J. E. Sohn, G. D. Stucky, Eds., American Chemical Society, Washington D.C. 1991, p. 279
3. R. J. Jeng, Y. M. Chen, J. J. Chen, J. Kumar, S. K. Tripathy, *Macromolecules* **26**, 25, (1993)
4. R. Levenson, J. Liang, J. Zyss *Polym. Prepr.* **35**(2), 162 (1994)
5. H.-Q. Xie, Z.-H. Liu, H. Liu, J-S Guo, *Polymer* **39**(12), 2393 (1998)
6. A. Hult, F. Sahlén, M. Trollsås, S. T. Lagerwall, D. Hermann, L. Komitov, P. Rudquist, B. Stebler, *Liquid Crystals* **20**, 23 (1996)
7. M. Trollsås, C. Orrenius, F. Sahlén, U. W. Gedde, T. Norin, A. Hult, D. Hermann, P. Rudquist, L. Komitov, S. T. Lagerwall, J. Lindström, *J. Am. Chem.Soc.*, **118**, 8542 (1996)
8. F. Sahlén, M. Trollsås, A. Hult, U. W. Gedde, D. Hermann, P. Rudquist, L. Komitov, S. T. Lagerwall, *Polymer Prepr.* **38**, 979 (1997)
9. M. Lindgren, J. Örtegren, P. Busson, A. Eriksson, D.S. Hermann, A. Hult, U. W. Gedde, P. Rudquist, S.T. Lagerwall, *SPIE*, **3475**, 76 (1998)
10. V. G. Dmitriev, G. G. Gurzadyan, D. N. Nikogosyan, *Handbook of Nonlinear Optical Crystals*, Second Edition, Springer Verlag Berlin 1997.
11. J. F. Nye *Physical Properties of Crystals*, Clarendon Press, Oxford, 1957, pp. 116-130.
12. B. Park, M. Lim, J.-H. Lee, J. -H. Kim, S.-D. Lee, *Ferroelectrics*, **179**, 231 (1996)
13. M. Lindgren, D. Hermann, J. Örtegren, P.-O. Arntzén, U. W. Gedde, A. Hult, L. Komitov, S. T. Lagerwall, P. Rudquist, B. Stebler, F. Sahlén, M. Trollsås, *J. Opt. Soc. Am. B*, **15**, 2 (1998)
14. D. A. Kleinman, *Phys. Rev.*, **126**, 1977 (1962)
15. R. J. Gulotty, C. D. Hall, M. J. Mullins, A. P. Haag, S. E. Bales, D. A. Miller, C. A. Berglund, M. S. La Barge, A. J. Pasztor, Jr., M. A. Chartier, K. A. Hazard, *Polymer Prepr. (Am. Chem. Soc. Div. Polym. Chem.)*, **35**, 196 (1994)
16. K. T. Gillen, M. Celina, R. L. Clough, J. Wise, *Trends Polym Sci.*, **5**, 250 (1997)
17. A. Krupicka, J. Åberg, M. Trollsås, F. Sahlén, A. Hult, U. W. Gedde, R. H. Boyd, *Polymer*, **38**, 346 (1997)
18. Z.-Y. Cheng, S. Yilmaz, W. Wirges, S. Bauer-Gogonea, S. Bauer, *J. Appl. Phys.* **83**, 7799 (1998)